IEEE Access
Multidisciplinary ⋮ Rapid Review ⋮ Open Access Journal

Received 10 April 2024, accepted 6 May 2024, date of publication 14 May 2024, date of current version 23 May 2024.

Digital Object Identifier 10.1109/ACCESS.2024.3400896

RESEARCH ARTICLE

On the Impact and Mitigation of Turbulence in Fiber-Coupled FSO Systems

VITOR D. CORREIA, MARCO A. FERNANDES, (Member, IEEE), PAULO P. MONTEIRO, (Senior Member, IEEE), FERNANDO P. GUIOMAR, (Member, IEEE), AND GIL M. FERNANDES
Instituto de Telecomunicações, University of Aveiro, 3810-193 Aveiro, Portugal

Corresponding author: Vitor D. Correia (vitor.correia@av.it.pt)

This work was supported in part by Fundo Europeu de Desenvolvimento Regional (FEDER) through the CENTRO 2020 Programme by Fundação para a Ciência e Tecnologia (FCT)/Ministério da Ciência, Tecnologia e Ensino Superior (MCTES) through Project OptWire under Grant PTDC/EEI-TEL/2697/2021, in part by the Marie Sklodowska-Curie Actions (MSCA) Research and Innovation Staff Exchange (RISE) Programme through Project Deep Intelligent Optical and Radio Communication Networks (DIOR) under Grant 10100828, and in part by Optical Radio Convergence Infrastructure for Communications and Power Delivering (ORCIP) under Grant CENTRO-01-0145-FEDER-022141. The work of Gil M. Fernandes was supported by FCT through the Individual Scientific Employment Program under Contract 2022.07168.CEECIND.

ABSTRACT Fiber-coupled free-space optics (FSO) communications have emerged as a promising wireless technology due to their flexibility, speed, security, and seamless integration with fiber optic systems. However, these systems are very sensitive to atmospheric conditions, particularly turbulence, necessitating robust and tailored solutions according to the application scenarios. However, the intrinsic random nature of atmospheric turbulence, together with the strong dependence on multiple external factors (e.g. varying weather conditions), makes it extremely challenging to adequately compare the merit of different turbulence mitigation techniques. In this work, resorting to the use of a custom-made atmospheric chamber, we tackle the issue of turbulence-induced power fading employing two complementary optical mitigation techniques: i) through enhanced fiber coupling efficiency using either standard single-mode fiber (SSMF) or multi-mode fiber (MMF) and ii) through tailored optical pre-amplification using either Erbium-doped fiber amplifiers (EDFAs) or semiconductor fiber amplifiers (SOAs). By carrying out a comprehensive set of repeatable and inter-comparable turbulence emulation tests, we demonstrate that MMF-based fiber coupling can be highly advantageous for less demanding FSO links, achieving 100 % reliability after a real-time BER assessment at 4.5 Gbps over weak-to-moderate turbulence, which represents a major improvement over the ∼10-50% reliability obtained under the same circumstances for the SSMF-coupled system. In turn, for FSO links requiring high-capacity SSMF-coupled receivers, we demonstrate that EDFA-based pre-amplification operating either in saturation or automatic power control (APC) enabling 10 Gbps connectivity with 99 % reliability in weak turbulence and ∼96-98 % in moderate turbulence regimes, in contrast with the baseline reliability of unamplified systems in the same turbulence conditions, which have shown <50 % and <10 % reliability with weak and moderate turbulence, respectively. Although also highly effective in mitigating turbulence-induced power fades, SOA-based pre-amplification was found to fall short of its EDFA counterpart, mainly owing to its degraded noise figure and nonlinear response, leading to reliability performance in the range of ∼70-90 %, over the same turbulent conditions.

INDEX TERMS Optical wireless communications, free-space optics, fiber coupling, atmospheric turbulence mitigation, optical pre-amplification.

I. INTRODUCTION

Free-space optics (FSO) communications have recently emerged as a promising solution for the future of wireless transmission communications. FSO refers to the transmission of modulated Infrared (IR) beams through the atmosphere, or vacuum [1]. The main advantages of FSO are associated with its resistance to electromagnetic interference, wide unregulated spectrum, and virtually unlimited bandwidth. In addition, by employing free-space-to-fiber coupling, this

The associate editor coordinating the review of this manuscript and approving it for publication was Stefan Schwarz.

technology can be easily integrated with current fiber optic networks, enabling the delivery of Tbps capacities [2] in a cost-efficient way, exploring mature, low-cost, and high-energy-efficient fiber-based optical components.

Despite its prominent advantages, FSO communications also face some technical challenges, including beam divergence over long distances, pointing errors, significant atmospheric attenuation in adverse weather conditions (fog, snow, and rain), and turbulence in the atmosphere. While there are effective practical solutions to the challenges of divergence, steering, and attenuation, the issue of power fading induced by atmospheric turbulence remains largely unresolved and has been the subject of much research [10]. Thereby, the experimental mimicry of atmospheric turbulence in a controllable way can help understand their impact on optical communications as well as in the development of mitigation techniques. Turbulence emulation approaches based on wavefront distortion have been employed to analyze the coupling efficiency, but these systems, usually based on spatial light modulators (SLM), tend to operate at a few Hz [11]. On the other hand, atmospheric chambers enable the emulation of the dynamic time response of atmospheric turbulence by creating strong temperature gradients inside the chamber [12]. In that way, atmospheric chambers enable the experimental modeling of atmospheric turbulence taking into account its characteristic time response, thereby enabling an accurate real-time performance assessment of the FSO communication system.

Resorting to atmospheric chambers, the performance of FSO communications systems had been characterized under several turbulent regimes, as well as the performance of different mitigation techniques [13]. At the digital signal processing (DSP) level, adaptive data rate techniques or enhanced forward error correction (FEC) approaches have been recently proposed to mitigate the impact of turbulence [14]. Despite their effectiveness, these solutions typically lead to an overall constraining of the system capacity [15]. In turn, while optical subsystems tend to keep the system capacity constant, they also tend to be more costly, such as wavefront correction based on adaptive optics [16], pointing, acquisition, and tracking (PAT) mechanisms [17] or multiple-input multiple-output (MIMO) systems that require multiple optical heads at the transmitter and receiver sides [18]. Another approach involves the exploitation of enhanced fiber coupling approaches, which can comprise few-mode fibers (FMF) or multi-mode fibers (MMF) [4]. These fibers tend to enhance the fiber coupling because the distorted wavefront can be coupled on other modes, with different spatial distributions, than the fundamental mode. Furthermore, fibers with larger core sizes and numerical apertures are more resistant to beam wandering and can couple more light. It has been studied that larger core fibers tend to be more resilient, increasing the coupling efficiency [5], [19]. When compared with standard single-mode fiber (SSMF) coupling, in [4] a gain of 49% and 39% in terms of coupled power was reported for 2-mode and 4-mode fibers, respectively, in channels affected by moderate and strong turbulence regimes. Although the FMF approach using mode division multiplexing (MDM) can boost the system performance and capacity, this tends to require several coherent receivers assisted by MIMO DSP [20]. On the other hand, the use of MMF at the receiver side emerges as a very appealing solution to improve the resilience of FSO systems in a cost-efficient way [5].

However, due to the impact of multi-modal dispersion, their performance can deteriorate the signal quality. In [21] and [22], the reported results show a decrease in bit error rate (BER) performance and tolerance to FSO link misalignment as the MMF length is increased, and therefore this solution is not suitable when the receiver is far away from the optical head. In addition, MMF coupling is not compatible with current fiber optic networks based on SSMF.

An alternative approach to compensate for the deleterious effect of turbulence-induced power fading involves the dynamic compensation of optical losses by an optical amplifier. Usually, this compensation happens on the receiver side, i.e., pre-amplification [23], [24], but it can also be complemented by dynamic power compensation on the transmitter side to mitigate slow fading effects [25]. When discussing optical amplification systems, it is crucial to compare the performance provided by Erbium-doped fiber amplifiers (EDFAs) and semiconductor optical amplifiers (SOAs). In [9], the authors evaluated the BER performance, of a signal transmitted at approximately 1 Gbps, considering different optical pre-amplification approaches, including EDFA and SOA in saturation, under different turbulence conditions generated by an atmospheric chamber. Despite the merits of optical pre-amplification schemes, they contribute with added noise and also increase the cost and power consumption of communication systems. Therefore, the design of efficient optical mitigation strategies to reduce the impact of turbulence is a non-trivial challenge that deserves further research. To that end, the realization of experiments in controlled but realistic laboratory environments is a key requisite to enable a consistent and repeatable comparison of available turbulence mitigation options.

In this paper, the performance of two optical mitigation techniques for turbulence-induced power fading in fiber-coupled FSO communication systems is comprehensively characterized. This characterization considers the evaluation of power fading and the real-time performance assessment of BER under different atmospheric conditions recreated by an atmospheric chamber, allowing a more complete and detailed study in relation to existing works in the literature, as shown in Table 1. In the first mitigation scheme, MMF is used at the receiver side of the FSO link, providing 100 % reliability in moderate turbulence. This results in a reliability gain of around ∼40% in weak turbulence regimes, and a gain of ∼90% in moderate turbulence regimes over the traditional approach with SMF-based coupling. The

TABLE 1. Main works on fiber coupling and pre-amplification for atmospheric turbulence mitigation in the literature.

	Fiber Coupling	Pre-amplification Scheme	Bit Rate p/ Channel (Gbps)	Atmospheric Turbulence Emulator	Real-time Assessment
[3]	3-mode fiber	-	40	SLM (weak-to-strong turbulence)	No
[4]	SSMF 2-mode fiber 4-mode fiber	-	CW	SLM (weak-to-strong turbulence)	No
[5]	SSMF (200 μm & 600 μm)	-	CW	Outdoor scenario (weak-to-moderate turbulence)	No
[6]	SSMF MMF (50 μm)	-	10	Atmospheric Chamber (weak turbulence)	Yes
[7]	6-mode fiber	6-mode EDFA	96	Heaters and fans (turbulence not explicitly reported)	No
[8]	SSMF	EDFA in saturation	40	Outdoor scenario (only weak turbulence)	Yes
[9]	SSMF	EDFA/SOA in saturation	1.244	Atmospheric chamber (only weak turbulence)	Yes
Our work	SSMF MMF (50 μm)	EDFA/SOA in saturation EDFA with APC mode	4.5 / 10	Atmospheric chamber (weak-to-strong turbulence)	Yes

second approach involves pre-amplification schemes (using EDFA and SOA) in different operation modes, saturation, and automatic power control (APC), which provides the best solution, achieving a reliability of ∼98-99 % over weak-to-moderate turbulence: compared to the unamplified solution, leading to gains of ∼60 % in weak turbulence regimes, increasing up to ∼90 % in moderate turbulence regimes. By using an EDFA in APC mode and comparing its performance against saturated EDFAs and SOAs, in this work we take an innovative approach for the mitigation of strong turbulence effects, backed up by a comprehensive real-time assessment of their respective BER performances.

The remainder of this paper is organized as follows. In section II, the utilized atmospheric chamber is presented and characterized over different turbulence levels. In section III, the gains provided by MMF coupling are evaluated in terms of power and system reliability in different turbulence conditions. In section IV, the performance of different mitigation techniques based on pre-amplification is characterized. Finally, in section V, the main conclusions are presented.

II. TURBULENCE EMULATION USING AN ATMOSPHERIC CHAMBER

Atmospheric chambers have been extensively employed in scientific literature to mimic the natural conditions of the Earth's atmosphere for optical transmission. These chambers allow for the recreation and control of environmental variables that impact the optical transmission, such as temperature, humidity, and pressure. Doing so makes

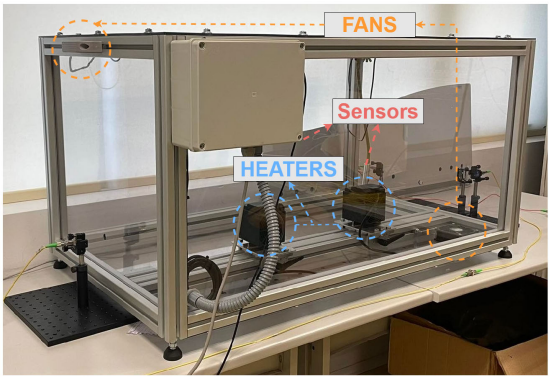

FIGURE 1. Custom-made atmospheric chamber used to generate weak-to-strong atmospheric turbulence.

it possible to conduct experiments under controlled and repeatable conditions to better understand the behaviour of optical wireless transmission in outdoor scenarios. Typically made of acrylic or glass walls, an atmospheric chamber usually contains a set of heaters, fans, humidity generators, smoke emulators, and monitoring sensors. Overall, the length of these chambers ranges from 1 to 5 meters [26], and they can reach temperatures up to 60°C [27], inducing strong thermal gradients that can lead to the generation of moderate turbulence regimes [12]. Its main purpose is to carry out experiments in a controlled environment, producing different turbulence conditions [12], including fog [13], [26], [27], and emulating the propagation of a laser beam through kilometers of atmosphere in a compact laboratory space.

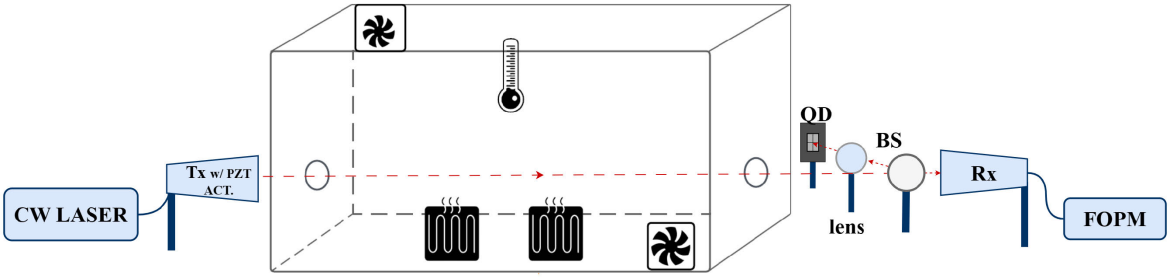

FIGURE 2. Experimental setup used to evaluate the performance of an FSO link under different atmospheric conditions generated in the atmospheric chamber.

The next subsections will present how we recreate outdoor optical wireless transmission inside a controlled laboratory environment, including the custom-made atmospheric chamber architecture, the characterization of the generated turbulence effects, and the decisive role played by automatic beam alignment in these systems.

A. CHAMBER DESIGN AND ARCHITECTURE

FIGURE 1 shows the atmospheric chamber employed in the following experiments, characterized by a length of 120 cm, 70 cm width, and 60 cm height.

It is equipped with two-time cycled heaters, which allow precise temperature control up to chamber temperatures of 70°C. The chamber is also equipped with two controllable fans that reach up to 9000 revolutions per minute (RPM). One fan injects air into the chamber while the other draws air out, resulting in rapid cooling when needed.

The conditions inside the chamber are monitored in real-time by two humidity and temperature sensors. As a whole, the chamber enables to create repeatable test environments, allowing precise temperature and cooling adjustments, while monitoring internal conditions in detail.

B. EXPERIMENTAL SETUP: FSO TRANSMISSION OVER A TURBULENT CHANNEL

The setup used for testing the impact of turbulence on the FSO transmission performance is illustrated in FIGURE 2. Two collimators, Thorlabs F810APC-1550, were used for the transmission/reception of the optical signal in free space. These collimators were positioned at a distance of 150 cm from each other. A continuous wave (CW) laser was directly connected to the Tx collimator, emitting at a wavelength of 1550 nm, with an optical power of 11 dBm. After the Rx collimator, a fast optical power meter (FOPM) is used to measure the collected optical power at sampling-rate of 10 kSps.

To keep the FSO link continuously aligned, we utilized a commercial PAT system, compensating for any pointing errors occurring during the experiments. The automatic alignment system employs two piezoelectric inertial actuators (Thorlabs PIAK10), attached to the transmitter collimator, an electronic driver (Thorlabs KIM101), a beam position aligner (Thorlabs KPA101), a 92/8 beam splitter (BS), which reflects part of the beam towards a quadrant detector (QD) (Thorlabs PDQ30C), by a plano-convex lens. This system allows for real-time monitoring and correction of the beam position, enabling continuous alignment to a set position through closed-loop control.

C. EXPERIMENTAL ASSESSMENT OF TURBULENCE-INDUCED POWER FADING AND POINTING ERRORS

To experimentally validate the capability of the chamber to generate realistic turbulence regimes, in this section we make use of the setup of FIGURE 2 in a progressive heating configuration, analyzing the statistical distribution of optical power over time. Furthermore, to assess the importance of adaptive beam alignment on the practical impact of turbulence, we consider two complementary experimental analyses: i) without adaptive beam alignment (i.e. with link alignment performed at room temperature, without any further adjustments) and ii) with adaptive beam alignment over time, attempting to correct any pointing error effects generated by turbulence. We started the aforementioned analysis by programming the atmospheric chamber to keep the heaters on (100% duty-cycle) for 18 minutes, resulting in temperatures exceeding 45°C, which was adjusted to provide high enough levels of turbulence. The evolution of temperature inside the chamber, as recorded by the installed temperature sensors, is depicted in FIGURE 3a, considering the scenarios with and without automatic beam alignment. The similarity of the obtained results evidences the repeatability of the atmospheric chamber, crucial to mimic practical outdoor conditions in a controlled laboratory environment.

FIGURE 3b shows the recorded beam position measured in the QD with and without beam alignment, on top of a heatmap of coupled power as a function of the incident beam position in the received collimator. As would be expected, without automatic beam alignment we observe a cumulative beam deviation from the optimal point that leads to the increased fixed coupling losses shown in FIGURE 3c. Here, we can observe that without beam alignment the losses due to pointing errors can rise up to 20 dB. On the other hand, with automatic alignment, the losses are contained below 5 dB.

Making use of the fast optical power meter sampling at a rate of 10 kSps, in FIGURE 4, we can see the

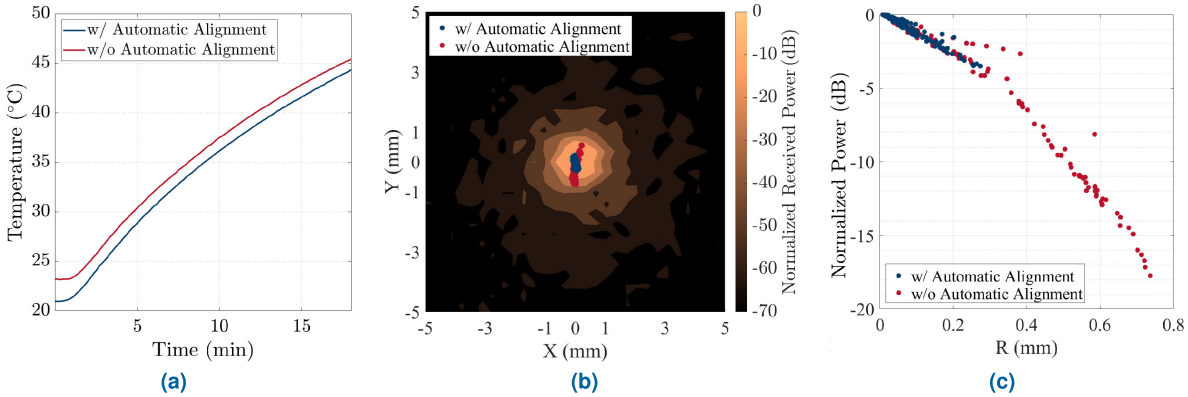

FIGURE 3. Recording of beam position and temperature during atmospheric chamber heating with and without automatic alignment. (a): Evolution of the temperature inside the atmospheric chamber for both approaches. (b): Beam position over time in a collimator lens. (c): Power losses as a function of the distance from the center of the collimator.

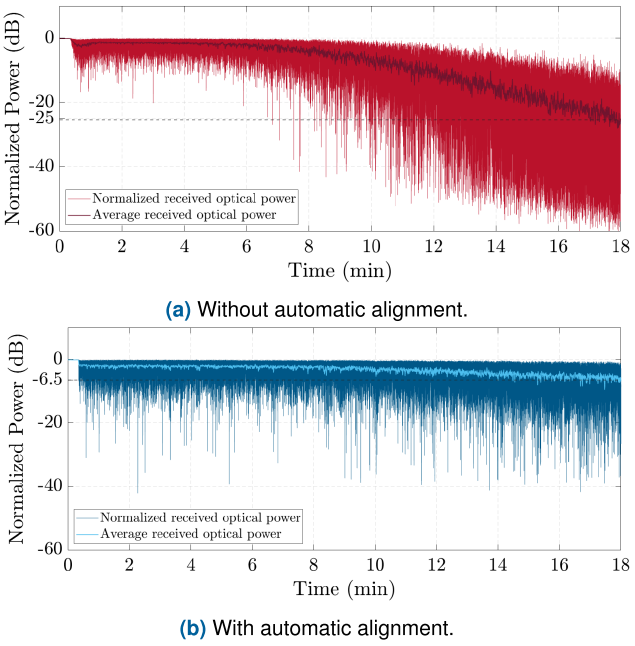

FIGURE 4. Evolution of the normalized received optical power under the influence of atmospheric turbulence generated inside the atmospheric chamber.

received optical power over time with and without automatic alignment. For each case, this figure also displays the average received optical power, calculated with a moving average of 0.8 seconds, directly related to the power losses caused by beam misalignment relatively to the center of the collimator, as shown in FIGURE 3c. The drop in average optical power of around 25 dB in FIGURE 4a, and around 6.5 dB in FIGURE 4b, can be explained based on the correlation between the power losses and the pointing errors observed during each test. Although it is expected that the losses in average optical power would correlate with the results shown in FIGURE 3c, the power losses are associated not only with pointing errors but also with the phenomenon of beam scintillation, which leads to an additional power loss of 3 dB and 7 dB for the systems with and without automatic beam alignment, respectively.

By analyzing the evolution of received optical power, it becomes clear that the rising temperature inside the chamber leads to increasing levels of turbulence, which directly manifests into the visible enhancement of power fadings. In addition to this effect, and following our previous discussion, the induced temperature increase also causes a reduction of the average refractive index of the air inside the chamber, thereby generating a slight refraction of the beam that leads to beam misalignment and consequent average power loss.

Following this issue, we have then activated the automatic beam alignment system, which enabled to realign the FSO link according to the temperature-induced refraction. This led to the beam remaining near the central position of the collimator, as shown in FIGURE 3b, thus significantly reducing the associated power loss of around 25 dB, without automatic alignment, to less than 6.5 dB (see FIGURE 3c). Naturally, owing to the stabilized average position of the received optical beam close the center of the receiver-end collimator, the effect power fadings caused by beam wandering is also visibly reduced.

Note that, while the magnitude of beam wandering effects is expected to remain unaffected (the utilized PAT is not fast enough to correct for these sub-ms effects), their induced power losses are much lower, since position fluctuations are now centered at the origin (i.e. at the optimum alignment point).

As a whole, the carried out analyses and obtained results clearly highlight the crucial role played by automatic beam alignment in FSO systems, not only in long-range field-trial settings but also for the accurate emulation of FSO systems using atmospheric chamber setups.

D. EXPERIMENTAL VALIDATION OF MULTIPLE TURBULENCE REGIMES

Exploiting the observed impact of progressive heating inside the chamber on the variation of optical power over time, in this subsection we aim to validate that the measured turbulence-induced fading respects the expected trends for

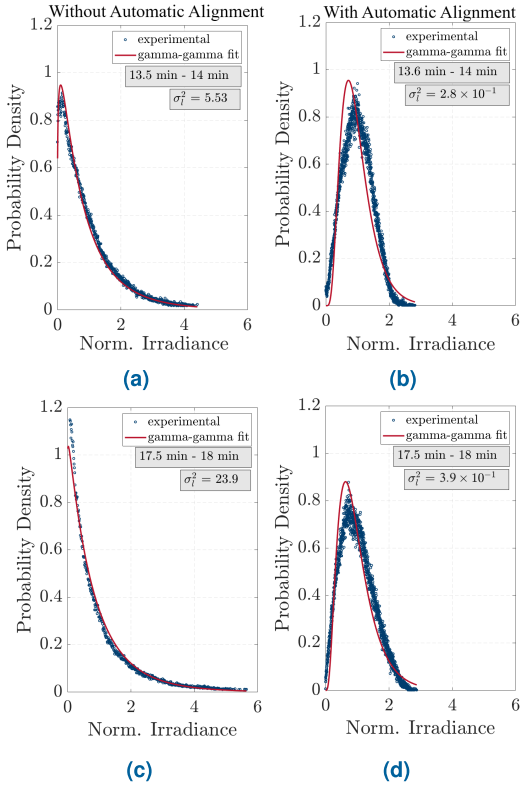

FIGURE 5. Experimental and theoretical (Gamma-Gamma) probability functions of the scintillation effect caused by atmospheric turbulence. (a), (c): without automatic alignment. (b), (d): with automatic alignment.

realistic FSO transmission scenarios. To that end, we now proceed with a comprehensive statistical treatment of the experimentally measured data, and its subsequent comparison against the well-known Gamma-Gamma model [28]. To quantify turbulence levels, Rytov variance (σ_l^2) is commonly used, which can be classified as weak, moderate, or strong [29]:

- weak-turbulence: $\sigma_l^2 < 0.3$;
- moderate-turbulence: $0.3 < \sigma_l^2 < 5$;
- strong-turbulence: $\sigma_l^2 > 5$.

Since the Rytov variance can be seen as a metric for the impact of turbulence, it is of paramount importance to discuss it in terms of the corresponding physical parameters. The expression for Rytov variance is given by [29]:

$$\sigma_l^2 = 1.23 C_n^2 k^{7/6} L^{11/6}, \tag{1}$$

where C_n^2 is the refractive index structure parameter, which is generally observed to range from about 10^{-13} to 10^{-16} $m^{-2/3}$, k is the wave number ($2\pi/\lambda$) and L is the channel path length.

Using the Gamma-Gamma model as a theoretical reference, FIGURE 5 shows the experimentally obtained probability density distributions and their best corresponding Gamma-Gamma fits (in a mean square error sense), with and without automatic beam alignment.

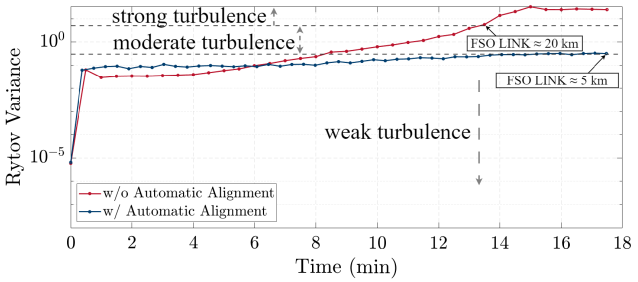

FIGURE 6. Comparison of the estimated Rytov variance from the fitting of the experimental data against a Gamma-Gamma model for a test with atmospheric turbulence with and without automatic alignment.

Both results are obtained for a fixed period of time of 30 seconds, after heating up the chamber. Two key observations can be extracted from these results: i) the histograms of experimentally collected data do follow the well-known asymmetric probability distribution that is characteristic of fading FSO channels, revealing a very good fit with the Gamma-Gamma function, and ii) the use of automatic beam alignment has a very relevant impact on the distribution of optical power, significantly lowering the measured Rytov variance from $>$ 5 (i.e. strong turbulence) to $<$ 1 (i.e. moderate turbulence).

These observations are corroborated by FIGURE 6, which shows the evolution of Rytov variance throughout the experiments with and without automatic beam alignment. From these results, we can observe that without automatic alignment, high values of Rytov variance (strong turbulence) are obtained, corresponding to the levels of turbulence obtained in FSO links of more than 20 km when assuming a typical value for the refractive index structure parameter of $C_n^2 = 10^{-15}$. However, after incorporating automatic alignment, lower turbulence values were observed, which resemble the turbulence obtained in links of around 5 km. It is important to note that this work only simulates atmospheric turbulence and does not take into account other effects in the atmosphere, such as absorption, scattering, and beam spreading.

As a good metric for measuring turbulence strength, it is common to use the Fried coherence length, which can be given by [30]:

$$r_0 = 1.68(C_n^2 L k^2)^{-3/5}, \tag{2}$$

where C_n^2 is the refractive index structure parameter, L is the length of the link, k is the wave number, $k = 2\pi/\lambda$, and λ is the wavelength. To determine the r_0 value for our system, we need to calculate the achieved C_n^2. Considering the maximum Rytov variance, $\sigma_l^2 = 5$, obtained in our 150 cm link, and using the equations (1) and (2), a minimum r_0 value of roughly 0.4 mm is determined, which falls within the range of values that are associated with strong atmospheric turbulence regimes, as reported in the literature [31].

III. FIBER COUPLING EFFICIENCY OF FSO SYSTEMS IMPAIRED BY TURBULENCE

The turbulence characterization performed in the previous section has been carried out employing fiber collimation into an SSMF, which is nowadays the most widely utilized fiber type in the majority of optical communication applications. However, the actual impact of turbulence on optical power fluctuation strongly depends on the characteristics of the fiber into which the signal is collimated. Namely, its core size and NA have an important influence on the air-to-fiber coupling efficiency [32]. Resorting to the graphical example of FIGURE 3b, it is easy to visualize that a fiber with a larger core will be more tolerant to beam wandering effects caused by atmospheric turbulence. In addition to higher tolerance to beam wandering, larger cores tend to decrease the impact of scintillation because more modes are supported, resulting in greater coupling efficiency under strong wavefront distortions [30].

To experimentally assess the role of optical fiber coupling on turbulent FSO systems, in this section we make use of the developed atmospheric chamber to generate repeatable turbulence regimes and thereby directly compare the measured optical power variations, and the BER performance when employing different fiber types at the receiver side.

A. EXPERIMENTAL SETUP

The experimental setup employed in this work to access the impact of turbulence with different fiber-coupled receivers is depicted in FIGURE 7. The optical signal, generated at 1550 nm by a directly modulated laser (DML, OCLARO TTA) was modulated at 4.5 Gbps by an RF signal from a BERT (Keysight M8041A). The signal is then launched into the atmospheric chamber, collimated in the fiber, and finally detected by a low-cost multimode PIN diode with a bandwidth of 2.5 GHz, which sets the main limitation for the achievable bit-rate of 4.5 Gbps in this case. The received electrical signal returns to the BERT to be analyzed, enabling the evaluation of BER in real-time over data batches of 200 ms. We repeated the atmospheric chamber heating test, in which the heaters ran continuously for 18 minutes. Two different fiber types are compared. i) an SSMF, characterized by a core diameter of 9 μm and ii) an NA of 0.14, and an MMF, characterized by a core diameter of 50 μm and an NA of 0.2.

B. EXPERIMENTAL RESULTS

FIGURE 8 presents the evolution of received optical power during the tests. It is evident that the MMF is remarkably more resilient to atmospheric turbulence than SSMF due to its larger core size and its multi-mode nature, which leads to a lower variation in optical power over time.

From the results we can observe that the MMF presents a maximum Rytov variance value of 4.5×10^{-3}, two orders of magnitude lower than the maximum Rytov variance value for SSMF of 3.3×10^{-1}, thus evidencing the advantages of larger core fibers. In general, fibers with a larger core diameter and NA also have the potential to couple more light, thus reducing the sensitivity to beam deviations, leading to a lower Rytov variance, as can be observed in FIGURE 8b. In addition to its strong resilience to power losses caused by beam wandering, the multi-mode nature of the fiber makes it more resilient to wavefront distortions associated with scintillation.

Since we obtained two quite different results, we decided to use two theoretical models to obtain the Rytov variance: the Log-Normal model which is more suitable for weak turbulence regimes, and the Gamma-Gamma model predominantly used in moderate and strong turbulence regimes [28].

To measure the communication performance of each approach, the real-time BER was measured. As a result of the BER measurements, reliability was used to evaluate the system's performance over time. Reliability was calculated by dividing the number of error-free batches by the total number of BER measurements. FIGURE 9 displays the BER measurements taken during two tests using either SSMF or MMF-based coupling. As predicted from the power results shown in FIGURE 8, the signal quality deteriorates over time due to atmospheric turbulence effects such as beam scintillation and beam wandering. Towards the end of the test, when the Rytov variance values are at their highest, as shown

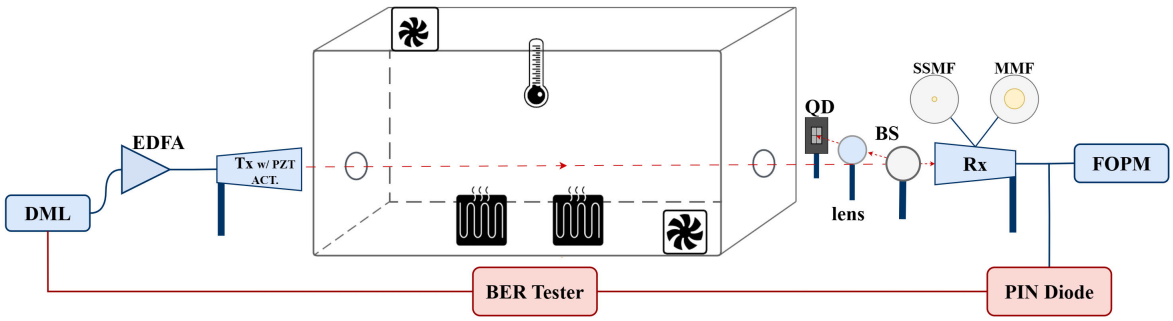

FIGURE 7. Schematic of the experimental setup used for real-time performance assessment of an FSO communication system under the impact of atmospheric turbulence with different fiber coupling approaches.

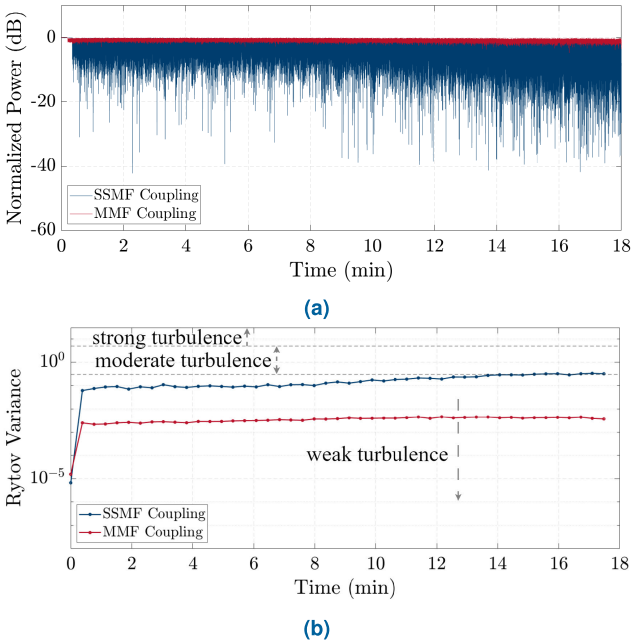

FIGURE 8. (a): Evolution of the normalized received optical power under the influence of atmospheric turbulence for SSMF and MMF coupling. (b): Comparison of the estimated Rytov variance from the fitting of experimental data against a Log-Normal and Gamma-Gamma theoretical reference for different fiber-coupling approaches.

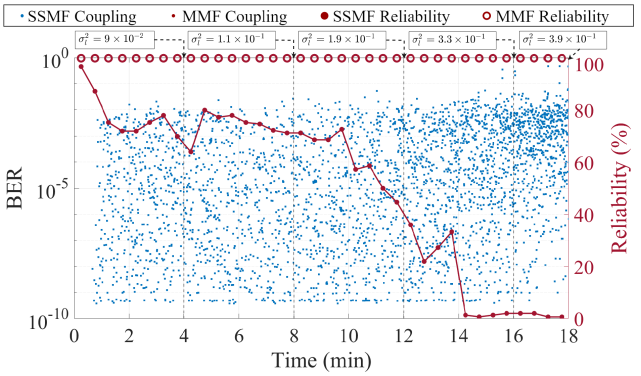

FIGURE 9. BER and reliability evolution for SSMF and MMF Coupling (4.5 Gbps).

in FIGURE 9, the BER values range from 10^{-6} to 10^{-4}, for the scheme with SSMF. On the other hand, MMF coupling remains error-free (note that the absence of MMF values in FIGURE 9 is due the logarithmic y-scale that prevents the representation of BER=0), providing a significant gain over SSMF due to its high coupling efficiency under turbulence.

During the whole experiment, the MMF-based solution presents full robustness to atmospheric turbulence, with a constant reliability of 100 %. However, when using SSMF with the same threshold (error-free), the reliability drops to 51%, even reaching zero reliability after reaching moderate turbulence regimes, making it sub-optimal for FSO communication systems under severe atmospheric turbulence.

In general, the obtained results clearly demonstrate that the use of MMF coupling can be highly beneficial to improve the performance of FSO systems impaired by moderate to strong turbulence, providing a low-cost mitigation strategy for multi-Gigabit optical wireless communications.

IV. MITIGATION OF TURBULENCE USING OPTICAL PRE-AMPLIFICATION

Whereas in the previous section, we have shown that MMF coupling can be highly effective in the mitigation of atmospheric turbulence in FSO systems, there are multiple application scenarios where the use of MMF-based receivers is not adequate or cannot be employed in practice. A couple of potential scenarios that are incompatible or challenging to implement MMF coupling are discussed in the following:
i) in fiber-wireless-fiber scenarios where the O/E conversion is located far away from the optical antenna, leading to signal propagation over several kilometers of fiber. In that case, the effect of multi-modal dispersion will quickly degrade the signal quality, eventually voiding the MMF coupling advantage after a few hundred meters.
ii) when targeting ultra-high-capacity FSO deployments, more advanced receiver paradigms are typically required, including the use of coherent optical receivers, whose baseline architecture involves the use of single-mode components, thereby preventing to benefit from the coupling advantages of MMF.

Conditioned by these challenges in these practical application scenarios, the use of SMF-based coupling might still be mandatory, thus an alternative technique for the mitigation of turbulence must be employed. Following this challenge, in this section, we exploit the developed atmospheric chamber to experimentally assess the turbulence mitigation capabilities provided by optical pre-amplification. In particular, following the unsettled discussion on this topic that can be found in the recent literature [9], [33], we aim to compare the FSO system performance using either EDFA or SOA pre-amplification. In addition, we also consider the amplification variants associated with operating the pre-amplifiers in saturation or with an APC loop. More specifically, three different approaches are employed to compensate for turbulence-induced signal loss:

- EDFA in saturation (model: EXELITE INNOVATIONS XLT-CF15);
- SOA in saturation (model: CIP Technologies SOA-S-OEC-1550);
- EDFA in APC mode (model: FS M6200-20BA).

In this experimental assessment, the performance of optical pre-amplification was evaluated in a 10 Gbps real-time transmission system.

A. EXPERIMENTAL SETUP

The experimental setup utilized to evaluate the performance of the considered optical pre-amplification strategies is depicted in FIGURE 10. At the transmitter side, a 10 Gbps

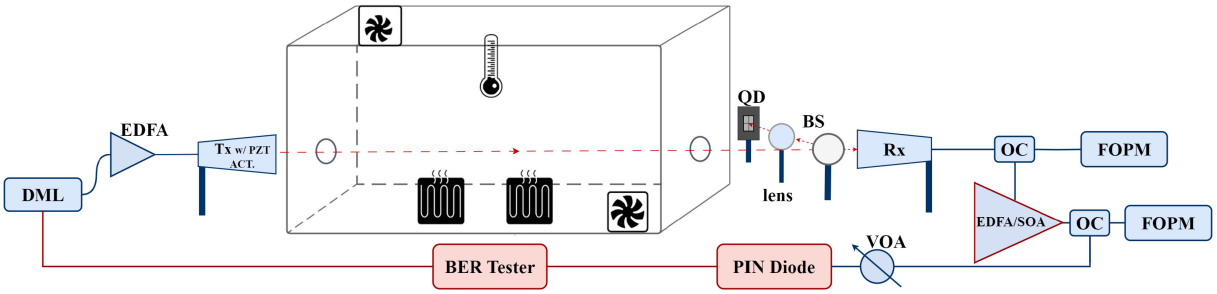

FIGURE 10. Schematic of the experimental setup used to test communications on an FSO link under atmospheric turbulence with a pre-amplification stage.

NRZ signal is generated using the previously introduced BERT. Note that, in this case, the data-rate has been set so that a fair comparison could be carried out between each of the pre-amplification approaches. After signal generation, a similar setup to the one described in section III was used. At the receiver side, the optical signal is collimated and then the setup is modified to add the pre-amplification stage. The signal is coupled through an SSMF fiber, and two 3 dB optical couplers are used to monitor the power at the input and output of the amplifier, using optical power meters. After the amplifier, a variable optical attenuator (VOA) is employed to optimize the input optical power of the PIN diode, which is found at -3 dBm. As the experiments were conducted using SSMF, a single-mode PIN diode (Nortel PP-10G) with 10 GHz bandwidth was utilized. After the signal is converted from the optical to the electrical domain, it is sent back to the BERT for analysis.

B. EXPERIMENTAL RESULTS

To assess the performance of each pre-amplification methodology, we repeated the previous test while measuring the optical power before and after compensation and the BER of the latter one. In FIGURE 11, the output power for the three tests with pre-amplification is displayed.

Overall, when comparing with the uncompensated signal, all implemented amplification methodologies resulted in a cleaner signal with a significant reduction of power fluctuations. For the saturated amplifiers, power fluctuations in the input signal that do not exceed the defined saturation margin[1] of 15 dB are easily mitigated by the amplifiers. In turn, the obtained results with the EDFA in APC mode reveal a lower performance in mitigating the turbulence-induced power fading, which can be explained since the APC methodology relies heavily on the control loop and amplifier response, significantly constraining the overall methodology reaction time.

Based on the analysis of the Rytov variance evolution in the different pre-amplification schemes, shown in FIGURE 12, it can be concluded that saturated amplifiers perform better

[1]The saturation margin is the gap between the amplifier input power without turbulence and the saturated input power, ensuring that any power loss peaks below thus gap would be mitigated.

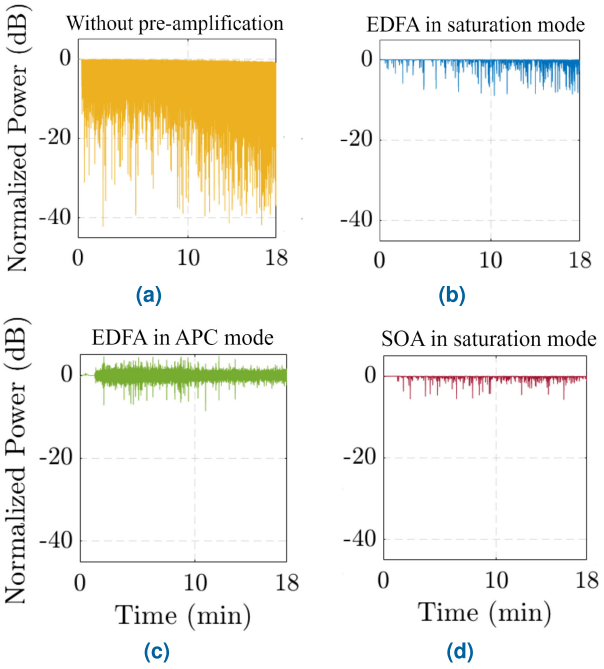

FIGURE 11. Evolution of the normalized received optical power under the influence of atmospheric turbulence for different pre-amplification approaches. (a): without pre-amplification. (b): EDFA in saturation mode. (c): EDFA in APC mode. (d): SOA in saturation mode.

in mitigating losses caused by atmospheric turbulence taking only into account a power stability criterion. The results show that pre-amplification significantly improves efficiency by equalizing turbulence-induced fading with reduced power variations.

In contrast to the analysis of received optical power, which demonstrates the superiority of saturated amplifiers, the BER measurements, shown in the FIGURE 13, indicate that the BER of the SOA-amplified system is significantly lower than the EDFA amplification, explained by the higher noise figure and non-linear response of SOAs. It is important to refer that, in a practical long-range FSO link, the impact of beam propagation losses (e.g. due to beam divergence and absorption) might typically require a dual-stage optical pre-amplification architecture, where the 1^{st} amplification stage should essentially compensate for the link loss, while the

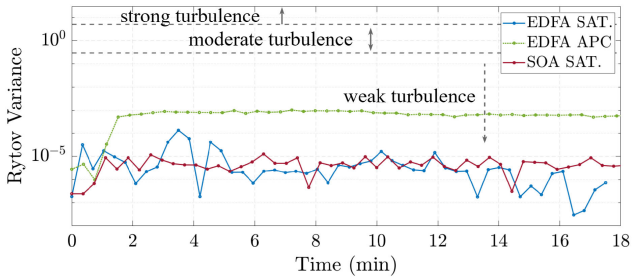

FIGURE 12. Comparison of the estimated Rytov variance from the fitting of the experimental data against a Log-Normal reference for different pre-amplification approaches.

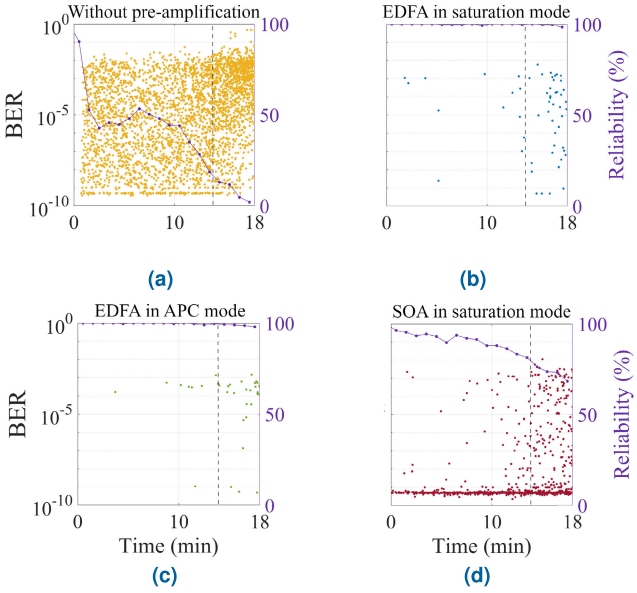

FIGURE 13. Comparison of the evolution of the BER performance for different strategies. (a) without pre-amplification; (b) EDFA in saturation mode; (c) EDFA in APC mode; (d) SOA in saturation mode. The vertical dashed line at 14 minutes represents the transition from weak to moderate turbulence regime.

2^{nd} stage can be designed to mitigate the turbulence effects. However, in this work, since we are mainly focused on the analysis of the turbulence mitigation capabilities provided by EDFAs/SOAs in the 2^{nd} amplification stage, the impact of the link loss has been neglected. Notably, the main challenge associated with the 1^{st} amplification stage lies on the SNR degradation caused by addition of amplified spontaneous emission (ASE) noise over a lower power received signal, which is mainly an engineering problem. In contrast, the 2^{nd} stage amplification studied in this work is not expected to significantly contribute to further SNR degradation since the input optical power at that stage should already be sufficiently high (> -25 dBm in this work).

To conclude, the obtained results have shown that both approaches are highly reliable, compensating for the large amount of (deep) fading caused by atmospheric turbulence. While the SOA displayed satisfactory power results, its introduction of noise to the system and its non-linear response leads to poorer performance than EDFAs. Nonetheless, SOA remains a viable option for this type of system as long as the transmission rate is adjusted and/or adequate non-linear mitigation measures are adopted. The EDFA in APC mode demonstrates exceptional performance, with reliabilities of 99%, responding quickly to power fluctuations caused by atmospheric turbulence. Furthermore, it produces exceptional outcomes while maintaining a low noise figure, which had no impact on the BER performance.

V. CONCLUSION

Atmospheric turbulence remains a critical bottleneck for terrestrial high-capacity outdoor optical wireless communications. This work tackled this challenge by proposing two approaches that considerably reduced this phenomenon: a passive approach relying on different fiber couplings and an active approach based on optical pre-amplification. Both approaches have been validated using an atmospheric chamber, reaching 4.5 Gbps and 10 Gbps, respectively. On the issue of fiber coupling enhancement, MMF coupling showed clear gains when compared with typical SSMF, showing strong resilience in scenarios of weak and moderate turbulence, with reliabilities of 100 % during the entire test, providing reliability gains of roughly 40 %, in weak turbulence regimes, and 90 % in moderate turbulence regimes, compared to SSMF. Targeting higher capacity scenarios, where SMF-coupling is mandatory, a pre-amplification technique using EDFAs and SOAs has been characterized. The EDFAs, in saturation and APC mode, have shown high efficiency in compensating for the power fading induced by turbulence, with reliabilities close to 100% in moderate turbulence regimes, especially the EDFA in APC, which has presented excellent results for a commercial amplifier. Table 2 summarizes the reliability values for the evaluated mitigation techniques, accounting for the different bit rates. Results show that both methods are effective strategies for power fading mitigation induced by atmospheric turbulence. Note that the reliability values indicated in Table 2 are obtained from end-to-end real-time BER measurements, and therefore already take into account the overall impact on system performance of the considered turbulence mitigation techniques, including

TABLE 2. Reliability for the different time windows of 5 minutes, and their respective maximum Rytov variance values achieved $\sigma_I^2 = 0.11$, $\sigma_I^2 = 0.23$, and $\sigma_I^2 = 0.39$, evaluated under different atmospheric turbulence conditions.

		Weak Turb.		Mod. Turb.
	R_b	≈ 2.5 km	≈ 3.75 km	≈ 5 km
	Gbps	$\sigma_I^2 = 0.11$	$\sigma_I^2 = 0.23$	$\sigma_I^2 = 0.39$
SSMF	4.5	74.2	58.2	8.40
MMF	4.5	100	100	100
W/o pre-amp.	10	48.3	39.9	9.30
EDFA sat.	10	99.8	99.8	96.7
SOA sat.	10	92.5	87.4	73.3
EDFA APC	10	99.9	99.6	98.3

potential associated penalties such as multi-mode dispersion (using MMF), ASE noise (using optical amplification) and nonlinearities (when using SOAs). Notwithstanding, it is worth emphasizing that the obtained results are tightly associated with the considered system parameters, such as bit-rate and transmission distance, and therefore their generalization to other system configurations should be carefully assessed.

In summary, EDFA in APC mode is a more interesting solution for very high-capacity scenarios that require integration with current fiber-optic networks. This solution enables the use of coherent detection with polarization multiplexing, targeting Tbps capacities, which could provide a significant capacity improvement of the system with the implementation of a wavelength division multiplexing (WDM) technique. However, with a WDM system, amplification must be distributed across different channels, potentially raising reliability issues on a per-channel level. On the other hand, for multi-Gigabit applications with the receiver placed very close to the optical head, MMF can be a more cost-effective solution with similar performance. Note that, whereas in this work the data-rate with MMF detection has been limited to 4.5 Gbps due to the narrow PIN bandwidth (2.5 GHz), there are currently other commercial multimode PIN receivers in the market that can potentially improve the available bandwidth and consequently the data-rate by a factor of 10-20 times [34]. Therefore, using state-of-the-art components, it is reasonably conceivable to achieve 100 Gbps MMF-based solution for highly-reliable FSO transmission in the near future. As a whole, by resorting to the use of a custom-made atmospheric chamber ensuring repeatable and realistic turbulence conditions, this work has contributed to shine light into the relative merits of different turbulence mitigation techniques and their respective potential application scenarios.

REFERENCES

[1] P. K. Sahoo and A. K. Yadav, "A comprehensive road map of modern communication through free-space optics," *J. Opt. Commun.*, vol. 44, no. 1, pp. 1497–1513, Feb. 2024.

[2] A. Malik and P. Singh, "Free space optics: Current applications and future challenges," *Int. J. Opt.*, vol. 2015, pp. 1–7, Jan. 2015.

[3] D. Zheng, Y. Li, H. Zhou, Y. Bian, C. Yang, W. Li, J. Qiu, H. Guo, X. Hong, Y. Zuo, I. P. Giles, W. Tong, and J. Wu, "Performance enhancement of free-space optical communications under atmospheric turbulence using modes diversity coherent receipt," *Opt. Exp.*, vol. 26, no. 22, pp. 28879–28890, 2018.

[4] D. Zheng, Y. Li, E. Chen, B. Li, D. Kong, W. Li, and J. Wu, "Free-space to few-mode-fiber coupling under atmospheric turbulence," *Opt. Exp.*, vol. 24, no. 16, pp. 18739–18744, 2016.

[5] S. Arisa, H. Endo, M. Sasaki, Y. Takayama, R. Shimizu, and M. Fujiwara, "Coupling efficiency of LASER beam to multimode fiber for free space optical communication," *Proc. SPIE*, vol. 10563, Nov. 2017, Art. no. 105630Y.

[6] C. Lalani, A. Mathur, and N. Bhatia, "Experimental investigations on an FSO-fiber converged communication system under fog and turbulence," *Appl. Opt.*, vol. 63, no. 13, pp. 3674–3684, 2024.

[7] Y. Huang, H. Huang, H. Chen, J. C. Alvarado, N. K. Fontaine, M. Mazur, Q. Zhang, R. Ryf, R. Amezcua-Correa, Y. Song, Y. Li, and W. Min, "Free-space optics communications employing elliptical-aperture multimode diversity reception under anisotropic turbulence," *J. Lightw. Technol.*, vol. 40, no. 5, pp. 1502–1508, Mar. 1, 2022.

[8] E. Ciaramella, Y. Arimoto, G. Contestabile, M. Presi, A. D'Errico, V. Guarino, and M. Matsumoto, "1.28 terabit/s (32×40 Gbit/s) wdm transmission system for free space optical communications," *IEEE J. Sel. Areas Commun.*, vol. 27, no. 9, pp. 1639–1645, Dec. 2009.

[9] M. Abtahi, P. Lemieux, W. Mathlouthi, and L. A. Rusch, "Suppression of turbulence-induced scintillation in free-space optical communication systems using saturated optical amplifiers," *J. Lightw. Technol.*, vol. 24, no. 12, pp. 4966–4973, Dec. 2006.

[10] A. Trichili, M. A. Cox, B. S. Ooi, and M.-S. Alouini, "Roadmap to free space optics," *J. Opt. Soc. Amer. B, Opt. Phys.*, vol. 37, no. 11, p. A184, 2020.

[11] A. Jullien, "Spatial light modulators," *Photoniques*, vol. 101, pp. 59–64, Mar. 2020.

[12] A. Aldaihan, M. Ijaz, S. Ekpo, A. Gibson, Z. Ghassemlooy, K. Rabie, and B. Adebisi, "Experimental results on the mitigation of turbulence in free space optics using spatial diversity," in *Proc. 12th Int. Symp. Commun. Syst., Netw. Digit. Signal Process. (CSNDSP)*, Jul. 2020, pp. 1–5.

[13] A. N. Khan, S. Saeed, Y. Naeem, M. Zubair, Y. Massoud, and U. Younis, "Atmospheric turbulence and fog attenuation effects in controlled environment FSO communication links," *IEEE Photon. Technol. Lett.*, vol. 34, no. 24, pp. 1341–1344, Dec. 15, 2022.

[14] M. A. Fernandes, G. M. Fernandes, B. T. Brandão, M. M. Freitas, N. Kaai, A. Tomeeva, B. V. D. Wielen, J. Reid, D. Raiteri, P. P. Monteiro, and F. P. Guiomar, "4 Tbps+ FSO field trial over 1.8 km with turbulence mitigation and FEC optimization," *J. Lightw. Technol.*, early access, Jan. 25, 2024, doi: 10.1109/JLT.2024.3358488.

[15] F. P. Guiomar, A. Lorences-Riesgo, D. Ranzal, F. Rocco, A. N. Sousa, M. A. Fernandes, B. T. Brandão, A. Carena, A. L. Teixeira, M. C. R. Medeiros, and P. P. Monteiro, "Adaptive probabilistic shaped modulation for high-capacity free-space optical links," *J. Lightw. Technol.*, vol. 38, no. 23, pp. 6529–6541, Dec. 2020.

[16] M. Vorontsov, T. Weyrauch, G. Carhart, and L. Beresnev, "Adaptive optics for free space laser communications," in *Proc. Appl. Lasers Sensing Free Space Commun.*, 2010.

[17] S. A. Al-Gailani, M. F. Mohd Salleh, A. A. Salem, R. Q. Shaddad, U. U. Sheikh, N. A. Algeelani, and T. A. Almohamad, "A survey of free space optics (FSO) communication systems, links, and networks," *IEEE Access*, vol. 9, pp. 7353–7373, 2021.

[18] M. A. Fernandes, P. P. Monteiro, and F. P. Guiomar, "400G MIMO-FSO transmission with enhanced reliability enabled by joint LDPC coding," in *Proc. Eur. Conf. Opt. Commun. (ECOC)*, Sep. 2021, pp. 1–4.

[19] S. A. Tedder and B. Schoenholz, "Study of lateral misalignment tolerance of a free space optical link for the development of an intra ISS point to point wireless optical link," in *Proc. 34th AIAA Int. Commun. Satell. Syst. Conf.*, Oct. 2016.

[20] Y. Weng, X. He, and Z. Pan, "Space division multiplexing optical communication using few-mode fibers," *Opt. Fiber Technol.*, vol. 36, pp. 155–180, Jul. 2017.

[21] B. Schoenholz, S. Tedder, P. Millican, and J. Berkson, "Bit error rate performance on passive alignment in free space optical links using large core fibers," *Proc. SPIE*, vol. 10524, Feb. 2018, Art. no. 1052415.

[22] M. M. Freitas, M. A. Fernandes, P. A. Loureiro, P. P. Monteiro, F. P. Guiomar, and G. M. Fernandes, "Robust and cost-efficient FSO transmission using a multi-mode fiber-coupled receiver," *Opt. Continuum*, vol. 3, no. 2, p. 227, 2024.

[23] M. Fernandes, G. Fernandes, B. Brandao, M. Freitas, N. Kaai, B. Wielen, J. Reid, D. Raiteri, P. Monteiro, and F. Guiomar, "Unraveling 'fiber in the sky': Terabit capacity enabled by coherent optical wireless," *IEEE Commun. Mag.*, vol. 62, no. 3, pp. 40–46, Mar. 2024.

[24] M. Fernandes, G. Fernandes, B. Brandão, M. Freitas, N. K. Kaai, A. T. Tomeeva, B. D. W. Wielen, J. R. Reid, D. R. Raiteri, P. Monteiro, and F. P. Guiomar, "Achieving multi-terabit FSO capacity with coherent WDM transmission over a 1.8 km field trial," in *Proc. Eur. Conf. Opt. Commun.*, 2023, pp. 1238–1241.

[25] B. T. Brandão, M. A. Fernandes, G. M. Fernandes, N. Kaai, A. Tomeeva, B. van Der Wielen, J. Reid, D. Raiteri, F. P. Guiomar, and P. P. Monteiro, "100G FSO field trial with transmitter power adaptability using a LoRa feedback channel," *J. Opt. Commun. Netw.*, vol. 16, no. 3, p. 270, 2024.

[26] M. Ijaz, Z. Ghassemlooy, J. Pesek, O. Fiser, H. Le Minh, and E. Bentley, "Modeling of fog and smoke attenuation in free space optical communications link under controlled laboratory conditions," *J. Lightw. Technol.*, vol. 31, no. 11, pp. 1720–1726, Jun. 2013.

[27] G. D. Verma, A. Mathur, and P. K. Yadav, "Experimental investigation of FSO systems under the effect of atmospheric turbulence, heat, and fog," in *Proc. IEEE 33rd Annu. Int. Symp. Pers., Indoor Mobile Radio Commun. (PIMRC)*, Sep. 2022, pp. 499–502.
[28] S. R. Z. Ghassemlooy and W. Popoola, *Optical Wireless Communications: System and Channel Modelling With MATLAB*. Boca Raton, FL, USA: CRC Press, 2012.
[29] E.-M. Amhoud, B. S. Ooi, and M.-S. Alouini, "A unified statistical model for atmospheric turbulence-induced fading in orbital angular momentum multiplexed FSO systems," *IEEE Trans. Wireless Commun.*, vol. 19, no. 2, pp. 888–900, Feb. 2020.
[30] D. M. Benton, A. D. Ellis, Y. Li, and Z. Hu, "Emulating atmospheric turbulence effects on a micro-mirror array: Assessing the DMD for use with free-space-to-fibre optical connections," *Eng. Res. Exp.*, vol. 4, no. 4, Dec. 2022, Art. no. 045004.
[31] S. R. Lekshmi, D. N. Naik, and C. S. Narayanamurthy, "Fried's coherence length measurement of dynamic Kolmogorov type turbulence using the autocorrelation function," *J. Opt.*, vol. 24, no. 4, Apr. 2022, Art. no. 044010.
[32] *What are Optical Fiber Core Size, Mode Field Diameter and Numerical Aperture?* Fiber Optics for Sale CO (FOSCO), Jul. 2023.
[33] R. Hui and M. O'Sullivan, "Chapter 3—Characterization of optical devices," in *Fiber-Optic Measurement Techniques*, R. Hui and M. O'Sullivan, Eds., 2nd ed. Cambridge, MA, USA: Academic Press, 2023, pp. 297–446.
[34] OPTILAB. *40 GHz Linear InGaAs PIN Photodetector, Multimode Fiber*. Accessed: Apr. 6, 2024. [Online]. Available: https://www.optilab.com/products/pd-40-mm

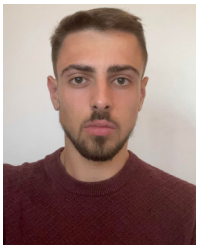

VITOR D. CORREIA received the M.Sc. degree in electronics and telecommunications engineering from the University of Aveiro, in 2023. During the M.Sc. degree, he worked with free-space optics (FSO) communications, studying and developing different techniques to mitigate atmospheric turbulence. He worked with different fiber-coupled schemes, including multi-mode fibers (MMFs) and multi-core fibers (MCFs) and also with optical amplifiers. He has already authored or coauthored two scientific publications in international conferences. He is a member of Optica.

MARCO A. FERNANDES (Member, IEEE) received the M.Sc. degree in electronics and telecommunications engineering from the University of Aveiro, in 2019, and the joint Ph.D. degree from the University of Aveiro, University of Porto, and University of Minho, through the MAP-Tele Doctorate Program, in 2023. During the M.Sc. degree, he worked with analog-radio over fiber applied to 5G communications. His Ph.D. degree was focused on high-capacity, reliable free space optics (FSO) communications exploiting coherent optics, advanced modulation techniques, and machine-learning-based channel estimation. Currently, he is a Postdoctoral Researcher participating in multiple research projects, mainly involving high-capacity FSO transmission for terrestrial and satellite applications. He has already authored or coauthored more than 40 scientific publications in leading international journals and conferences. He is a member of Optica. In 2021, he was a Finalist at the OFC2021 Corning Student Award, and in 2023, he was a Runner-Up at the ECOC Best Student Paper Award.

PAULO P. MONTEIRO (Senior Member, IEEE) is currently an Associate Professor with the University of Aveiro and a Senior Researcher with the Instituto de Telecomunicações, where he is also a Research Coordinator in optical communication systems (https://www.it.pt/Groups/Index/59) with the Instituto de Telecomunicações. His main research interests include optical communications, fixed mobile convergence, and reflectometry systems. Successfully tutored over 15 Ph.D.'s, 24 master's, and participated in more than 26 research projects. He has authored/coauthored more than 18 patent applications, over 157 articles in journals, and 290 conference contributions. He is a Coordinator of the Research Infrastructure.

FERNANDO P. GUIOMAR (Member, IEEE) received the M.Sc. and Ph.D. degrees in electronics and telecommunications engineering from the University of Aveiro, Portugal, in 2009 and 2015, respectively. Since 2017, he has been a Senior Researcher with the Instituto de Telecomunicações, Aveiro. He has authored or coauthored more than 150 scientific publications in leading international journals and conferences. His main research interests include fiber-based and free-space optical communication systems, including the development of digital signal processing algorithms, advanced modulation and coding, constellation shaping, and nonlinear modeling and mitigation. He is a member of OSA. In 2015, he has received a Marie Skłodowska-Curie Individual Fellowship, jointly hosted by the Politecnico di Torino, Italy, and CISCO Optical GmbH, Nuremberg. In 2016, he received the Photonics21 Student Innovation Award, distinguishing industrial-oriented research with high impact in Europe.

GIL M. FERNANDES received the degree in physics and in applied mathematics from the Faculdade de Ciências, University of Porto, in January 2008, and the M.Sc. degree in physics engineering and the Ph.D. degree in electrical engineering from the University of Aveiro, Portugal, in December 2010 and December 2018, respectively. Currently, he is a Researcher with the Instituto de Telecomunicações, Aveiro, where he has contributed as a member of the principal team in more than ten research and development projects and has coauthored more than 40 scientific publications in leading international journals and conferences. He has been a Lecturer with the Physics Department, University of Aveiro, since 2019, where he teaches courses related to optics and physics. His primary research interests include high-capacity fiber-optic and optical wireless communication systems, digital signal processing, and optical signal processing.